Journal of
Plankton Research

academic.oup.com/plankt

J. Plankton Res. (2023) 45(1): 37–51. First published online December 15, 2022 https://doi.org/10.1093/plankt/fbac068

ORIGINAL ARTICLE

Concurrent observations of the euphausiid *Thysanoessa raschii* in an Icelandic fjord by acoustics and Video Plankton Recorder: comparisons with theoretical models of target strength

PALL REYNISSON[1,*], **ASTTHOR GISLASON**[1] **AND GARETH L. LAWSON**[2,†]

[1]MARINE AND FRESHWATER RESEARCH INSTITUTE, PELAGIC DIVISION, FORNUBUDIR 5, HAFNARFJORDUR 220, ICELAND AND [2]BIOLOGY DEPARTMENT, WOODS HOLE OCEANOGRAPHIC INSTITUTION, 86 WATER ST, FALMOUTH, MA 02543, USA

*CORRESPONDING AUTHOR: palli.breyniss@gmail.com

†PRESENT ADDRESS: GARETH L. LAWSON, CONSERVATION LAW FOUNDATION, BOSTON, MA 02110, USA

Received May 4, 2022; editorial decision September 10, 2022; accepted October 23, 2022

Corresponding editor: Marja Koski

In two surveys in an Icelandic fjord, September 2016 and October 2018, the target strength (TS) of the euphausiid *Thysanoessa raschii* was estimated at four frequencies (38, 70, 120, 200 kHz) by matching the acoustic backscatter to the number of euphausiids detected by a Video Plankton Recorder (VPR). Using forward-looking strobe lights on the VPR and doubling the towing speed lowered the estimated target strength by 4.3 dB. In 2016, the TS for euphausiids of mean length 20.7 mm averaged −98.4, −92.3, −86.6 and −82.8 dB at 38, 70, 120 and 200 kHz frequencies, respectively. In 2018, TS for euphausiids of mean length 19.9 mm averaged −98.2 dB at 38 kHz and −88.3 dB at 120 kHz. Theoretical modeling using a Distorted-Wave Born Approximation-based approach was used to compute the average target strength for the observed length distributions and for several density and sound speed contrast (*g*, *h*) and orientations. Except at 38 kHz, these results are in reasonable agreement with the TS estimated from the VPR-acoustic comparisons. The methodological approach presented provides an alternative to net-acoustic comparison or modeling for the estimation of euphausiid target strength.

available online at academic.oup.com/plankt

KEYWORDS: target strength; Video Plankton Recorder; euphausiids; avoidance; scattering properties; target classification

INTRODUCTION

As in several other regions in the North Atlantic, euphausiids play an important role in the marine ecosystem around Iceland as conveyors of matter and energy from primary producers to fish, seabirds and marine mammals. Four euphausiid species are common around Iceland. *Thysanoessa inermis* is common on the shelves all around the island, *T. longicaudata* is generally most abundant in the offshore areas and *Meganyctiphanes norvegica* over the shelf slopes, whereas *T. raschii* is prevalent in the fjords off the west, north and east coasts of Iceland (Einarsson, 1945; Silva *et al.*, 2016; Gislason, unpublished). Due to the important trophic role of euphausiids in the Icelandic marine ecosystem, systematic monitoring of euphausiid distribution and abundance has been part of the Marine and Freshwater Research Institute's annual monitoring program of hydrography, nutrients and plankton around the island since 2011 (Reynisson and Gislason, 2015).

One of the longest time series of routine acoustic surveying for mapping the distribution and abundance of euphausiids is for Antarctic krill (Hemple, 1983; Hewitt and Demer, 1993, 2000; Brierley *et al.*, 1998; Everson, 2000; Reiss *et al.*, 2008). In the northern hemisphere, numerous acoustic investigations of euphausids have been reported (Sameoto, 1980; Falk-Petersen and Kristensen, 1985; Simard and Lavoie, 1999; Coyle, 2000; Everson *et al.*, 2006), and there is increasing interest in conducting such surveys on a routine basis (Ressler *et al.*, 2005). Application of acoustic techniques has been central to the monitoring program for euphausiids in Icelandic waters since 2011 (Reynisson and Gislason, 2015).

A general concern when estimating the abundance of euphausiids by acoustic surveying lies in estimating the target strength (TS) of the krill, which is crucial to the conversion of the acoustic backscatter to biomass. Considerable uncertainty has prevailed around this parameter, and much effort has been put into describing and characterizing its attributes. For many years, the semi-empirical target strength model of Greene *et al.* (Greene *et al.*, 1991) was employed, but subsequently substantial progress has been made in the theoretical, physics-based modeling of the target strength of zooplankton (McGehee *et al.*, 1998; review by Stanton and Chu, 2000; Lawson *et al.*, 2006; Conti and Demer, 2006 and references therein).

Acoustic measurements on krill in captivity have been used to ascertain the variables of importance in describing the echo strength observed, e.g. behavior, material properties and shape (Foote *et al.*, 1990; Wiebe *et al.*, 1990; Demer and Martin, 1995, Miyashita *et al.*, 1996; McGehee *et al.*, 1998; Martin Traykovski *et al.*, 1998; Pauly and Penrose, 1998; Calise and Knutsen, 2012). Considerable effort has been made to measure those variables, either in captivity or *in situ* (Foote *et al.*, 1990; Chu and Wiebe, 2005; Lawson *et al.*, 2006; Smith *et al.*, 2010; Kubilius *et al.*, 2015; Sakinan *et al.*, 2019; Lucca *et al.*, 2021).

One approach in estimating target strength *in situ* has been to scale acoustic backscatter by measurements of abundance made via other means, typically nets, and comparing to theoretical models (Sameoto *et al.*, 1993; Simard and Sourisseau, 2009; McQuinn *et al.*, 2013; Wiebe *et al.*, 2013). Underwater cameras have also been used for this purpose (De Robertis, 2001; Trevorrow *et al.*, 2005). In these studies, concurrent acoustic TS estimates are generally not reported and direct *in situ* target strength measurements using split-beam echo sounders are few (Hewitt and Demer, 1996; Klevjer and Kaartvedt, 2006; Lawson *et al.*, 2006). Resolving acoustic targets by the split-beam method requires low densities of krill within the acoustic observation volume. This is clearly demonstrated by Hewitt and Demer (Hewitt and Demer, 1996), and they include only measurements within 25 m range. Similarly, Klevjer and Kaartvedt (Klevjer and Kaartvedt, 2006) and Lawson *et al.* (Lawson *et al.*, 2006) limit their range to c. 13–15 m. Scaling the acoustic measurements via either nets or optic imaging is not hindered by this requirement of low density, rather the opposite, although the avoidance of the krill to the sampling device may be of real concern in that case (Sameoto *et al.*, 1993; Wiebe *et al.*, 2004, 2013).

Sampling for this study was conducted in Isafjord-deep, the largest fjord on the Vestfjord peninsula (Fig. 1). The fjord is well suited for ecological studies since it is a semi-enclosed ecosystem and important as nursing grounds for several fish species. For practical reasons, the fjord is also easily accessible, with a branch of the Marine and Freshwater Research Institute being in one of the fishing villages in the fjord. Systematic ecological studies of zooplankton in Isafjord-deep were initiated in the late 1980s (Astthorsson, 1990; Astthorsson and Gislason, 1991, 1992). The earlier ecological studies in the fjord have shown that the seasonal cycle of plankton growth and development is characterized by phytoplankton spring blooming in April–May followed by the highest

biomass of mesozooplankton in August (Astthorsson and Gislason, 1992). Astthorsson (Astthorsson, 1990) examined the population dynamics of the three euphausiids in Isafjord-deep, *T. raschii, T. inermis* and *M. norvegica*. He found *T. raschii* to be the most abundant euphausiid in the fjord (65% of the total number of euphausiids), having a life span of just over 2 years, with the main spawning being closely related to the phytoplankton spring bloom.

The aim of this paper is to estimate the target strength of the euphausiid *T. raschii* by comparing the acoustic data at several frequencies with concurrent optic imaging by a Video Plankton Recorder (VPR). The acoustic backscatter scrutinized as euphausiids based on the acoustic frequency response and the abundance of euphausiids derived from the VPR tows are then matched in order to estimate the average target strength. Related to this, the effect of the VPR towing speed is investigated, as well as the effect of using forward-looking strobe lights on the VPR. The results are compared to theoretical modeling of target strength.

MATERIAL AND METHODS

Two 5-day surveys, in mid-September 2016 and late October 2018, were carried out in Isafjord-deep, (Fig. 1), to study the abundance and distribution of the euphausiid populations in the fjord. A local fishing boat, 17 m long (Valur IS-20), was used in 2016 and a 56-m trawler type research vessel (Bjarni Saemundsson RE-30) in 2018. Layers of varying densities of euphausiids were acoustically observed throughout the area. Biological sampling with nets confirmed that three species of euphausiids were most abundant in these layers, *T. raschii*, *M. norvegica* and *T. inermis*. In the inner part of the fjord these layers were more consistent and often quite dense, with *T. raschii* dominating. These conditions of dense layers of mostly monospecific composition were judged to be well suited for the comparison of the acoustic and optic measurements. All data obtained for this study were sampled during daylight hours when the euphausiids stayed relatively deep in the water columns and when mixing with other organisms and diel vertical migration from depth to surface or vice versa was believed to be minimal.

Study site

The area surveyed within the fjord was 320 km^2 with a maximum depth of c. 150 m. A trough with a depth of 90–140 m extends from the mouth of the fjord almost to the innermost part. The slopes on either side of the main trough are generally quite steep. The vessels steamed along more or less predefined tracks at a speed of 7–10 knots to acoustically map the distribution and abundance of the zooplankton in the area. Net sampling and VPR-tows were taken underway from time to time targeting acoustic features of interest. The VPR-acoustic comparison was carried out in the portion of the trough indicated in Fig. 1, where the euphausiids were most abundant.

Acoustic instrumentation

In 2016, four transducers, 38, 70, 120 and 200 kHz, were flush mounted on a wing-shaped plate at the end of a sturdy pole, which was fastened to the side of the boat with the transducer faces at 1 m below surface. In 2018, hull mounted transducers at 38 and 120 kHz with 5 m draft were available. All transducers were of the split-beam type and connected to EK60 GPT transceivers (Kongsberg Simrad). The echosounders were set to 2 transmissions per second using the power settings recommended by Korneliussen *et al.* (Korneliussen *et al.*, 2008). The relevant parameters for the acoustic equipment used during the surveys are listed in Table I. The on-axis sensitivities of the echosounders were calibrated on-site the day before or during the survey, using the appropriate copper spheres and a 38.1 mm diameter tungsten carbide standard target (Foote and MacLennan, 1984; Foote *et al.*, 1987). A measure of the acoustic volumes are the equivalent beam angles, alternatively beam widths, provided by the manufacturer according to tank measurements before delivery, and found in Table I.

Optic instrumentation

A Digital Autonomous Video Plankton Recorder (DAVPR) from Seascan Inc., equipped with a camera that takes color images at a rate of around 15 images per second, was used to estimate the abundance and tilt angle of the euphausiids (Davis *et al.*, 2004). The VPR was fitted with a SBE-49 Seabird CTD and Wetlabs ECO Puck fluorometer/turbidity sensor, by which temperature, salinity, depth and fluorescence were measured from essentially the same parcel of water where the images were taken. All sensors were mounted on a frame attached to the bottom of a 1.22-m V-fin depressor. The towing depth was monitored with a Scanmar depth sensor fitted on the wire just above the VPR. Each tow lasted 1–2 hours.

Four forward-looking strobe lights (Orcatorch D550) were fastened to the VPR frame. The light was produced by LED's with main color output between 420 and 650 nm. (CREE XM-L2 (U4)). Each light emits up to 1000 lumens at a strobe rate of 6 Hz. The tows were mainly targeted to the denser acoustic registrations

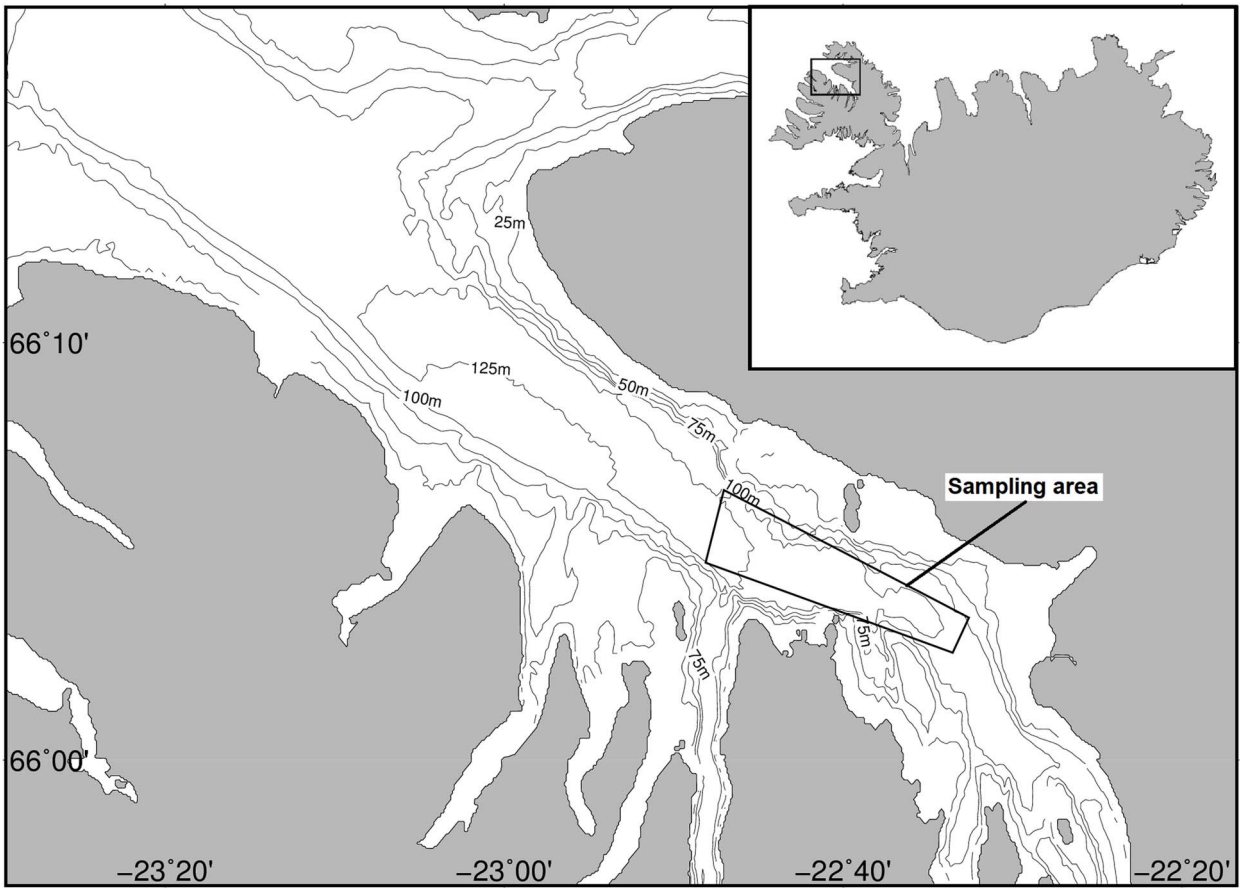

Fig. 1. Map of Isafjord-deep with the main sampling area indicated.

Table I: Main parameters of the transducers and transceivers of the EK60 echo sounders.

Year	Frequency	38 kHz	70 kHz	120 kHz	200 kHz
2016	Transducer type	ES38-12	ES70-7C	ES120-7	ES200-7C
	Power output (W)	500	750	250	120
	ψ (dB)	−15.8	−20.2	−20.8	−20.3
2018	Transducer type	ES38B		ES120-7	
	Power output (W)	2000		250	
	ψ (dB)	−20.7		−20.5	

ψ denotes the equivalent beam angle. A pulse length of 1 ms was used in all measurements.

identified as euphausiids. To investigate possible avoidance of the euphausiids to the VPR, several tows were made back and forth along the same transect having alternatively the forward-looking strobe lights on or off. For the same purpose, different towing speeds were also attempted (2 and 3.5 knots).

The VPR tows produced compressed data files of images as well as ancillary CTD and fluorescence data (Davis *et al.*, 2004; Hu and Davis, 2006). In-focus images of plankton/particles (Regions of Interest, ROIs) and environmental data were extracted from these files using the software AutoDeck (Seascan). For the present study, the field of view of the camera was set at 42 × 42 mm, giving a calibrated image volume of 407 mL. This value is a result from several calibrations carried out by Seascan in 2015, using thoroughly tested optic targets and at MFRI in 2016 using frozen *T. inermis* as a target.

The ROIs are time stamped to allow merging with the data from the CTD and the fluorometer that are written to separate data files. Upon starting the survey, the clocks

of the echosounder and the VPR were synchronized to the nearest second.

Biological sampling

It has been demonstrated that using strobe lights on plankton nets can greatly increase krill catch and may also affect the size distribution obtained (Sameoto *et al.*, 1993; Wiebe *et al.*, 2004; Wiebe *et al.*, 2013). This is believed to be due to reduced avoidance of the krill to the nets.

Euphausiid samples were collected using a 60-cm diameter Bongo net with 500-μm mesh size. To reduce avoidance, the net frame was equipped with four forward-looking strobe lights of the same type as used on the VPR (Gislason *et al.*, 2022). The net tows were generally targeted to the main layer of the euphausiids by towing at depths with the highest acoustic registrations (single net oblique-horizontal tow, type 10, Wiebe *et al.*, 2015). Several tows were made back and forth through the same acoustic layers using alternatively the forward-looking strobe lights on, 5 tows each year, or off, 4 tows in 2016 and 1 in 2018. The volume of water filtered by the net was measured with a HydroBios flowmeter. Length distributions of the euphausiids for tows with strobe lights off or on were determined separately.

The zooplankton samples were preserved in 4% neutralized formalin after collection. In the laboratory ashore, the samples were analyzed for euphausiid abundance and species composition. To obtain a manageable number for counting (c. 300 individuals counted), the samples were usually subsampled with a Motoda splitter (Motoda, 1959) before counting. In addition, the total length of a subset of individuals from each sample was measured, from the anterior edge of the eye to the tip of the telson excluding the setae (Mauchline and Fisher, 1969). Morphological measurements as described by Lawson *et al.* (Lawson *et al.*, 2006) were made on a subset of 32 individuals sampled by the Bongo net in each survey. The results from these measurements were used in the target strength modeling as described below.

Classification of euphausiid backscatter

The acoustic notation that follows is according to the convention described by MacLennan *et al.* (MacLennan *et al.*, 2002). The acoustic systems provided a continuous record of the volume backscattering from near-surface to below-bottom. The processing software LSSS 2.4.1(NORCE) was used to classify the echoes based on categorization either as emanating from euphausiids or other scatterers, using sample-validated data from the Bongo nets (Korneliussen and Ona, 2002; Korneliussen *et al.*, 2006). Active noise filtering was carried out as described by Korneliussen (Korneliussen, 2000). An offset of 0.5 m from the detected bottom was used in the processing. Manual editing of the data was performed to remove possible noise spikes from e.g. bottom and surface bubbles. Additionally, all data categorized as euphausiids with a difference in the mean volume backscattering strength at 120 and 38 kHz ($\Delta S_{v120-38}$) less than 5 dB were excluded to remove echoes from swimbladdered fish and other organisms with gas inclusions (Logerwell and Wilson, 2004; De Robertis *et al.*, 2010). Typical echograms at 120 and 38 kHz, as well as the 120 kHz data after masking everything but the euphausiid backscatter are shown in Fig. 2.

Analysis of VPR data

The total VPR towing time during this study was close to 14 hours in 11 tows in 2016 and 9 hours in 8 tows 2018. The images obtained by the VPR were analyzed automatically for abundance by the software Visual Plankton (Davis *et al.*, 2004; Hu and Davis, 2006), which employs a neural network trained with a set of ROIs of known, user-verified taxonomy, to classify ROIs to taxonomic category. All the automatic classifications were then examined and corrected for errors manually. The images were sorted into the following categories: euphausiids, copepods, marine snow, *Pseudocalanus* with egg sacs, chaetognaths, fish larvae, jellies and unknown. The resulting abundance numbers by the groups identified were output as averages per second.

From a sub-sample of images, the orientation of the euphausiids was estimated by measuring the angle of the long axis of the animals (head to tail) from the horizontal using a Matlab script as done by Lawson *et al.* (Lawson *et al.*, 2006). Only in-focus images of whole animals in side-view, plane to the camera, were considered for this exercise. An animal aligned perfectly horizontal was defined as having an angle of 0°, while animals facing upwards had positive angles and those facing downwards negative angles. These measurements were corrected by the average pitch of the VPR measured earlier under similar conditions, −3.0° with a 5.3° standard deviation, by a pitch and roll Data Storage Tag (Star-Oddi).

Estimation of target strength

The basis of the target strength estimation in this study relies on comparing the average number of euphausiids in a unit volume observed by the VPR to the concurrent average acoustic volume backscattering coefficient (s_v) along the VPR towing track. When matching the acoustic and optic data, the depth of the acoustic transducers and the time-lag between the observations by the echo

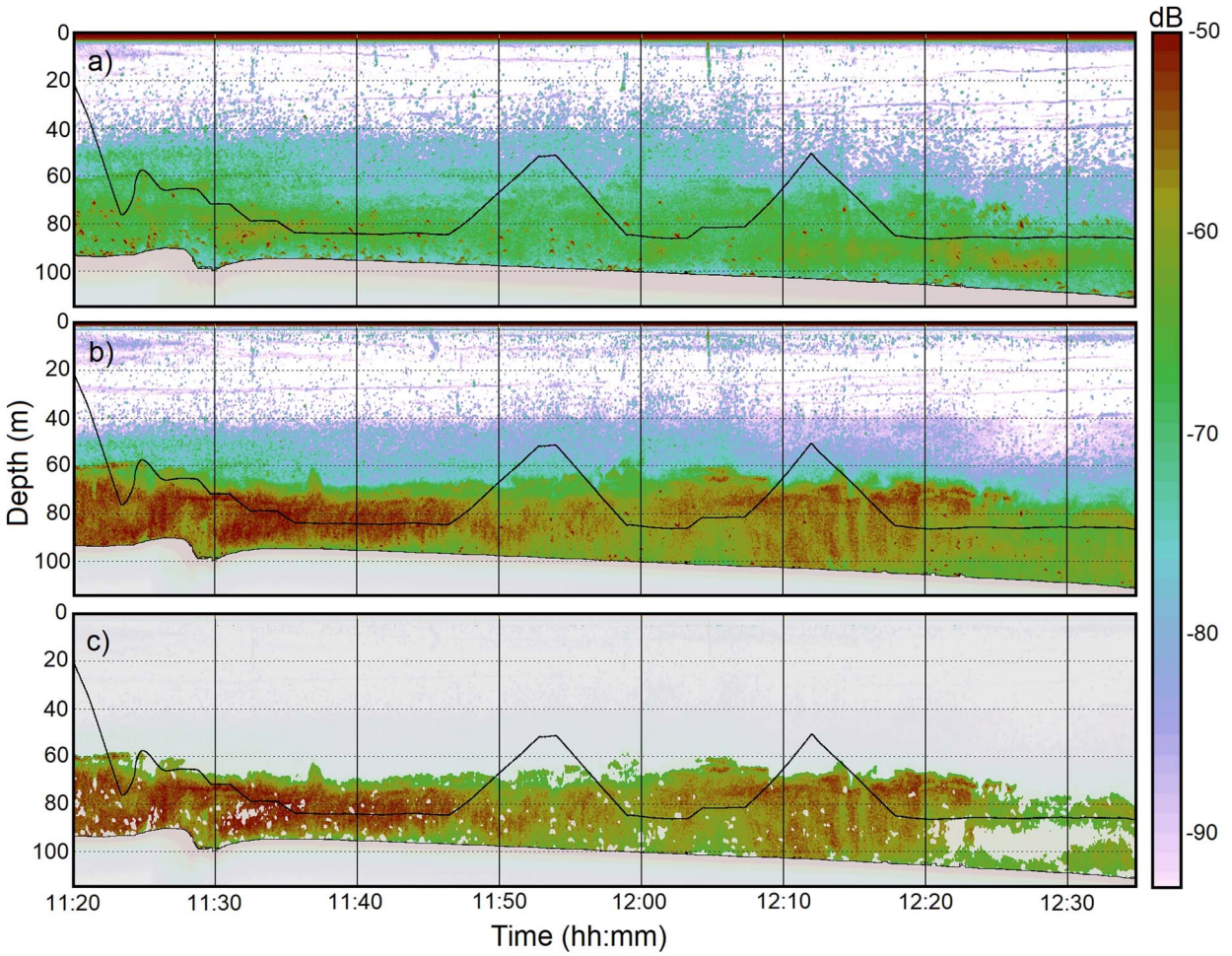

Fig. 2. Echograms from 16 September 2016, showing (**a**) unclassified S_v at 38 kHz and (**b**) 120 kHz, and (**c**) classified as euphausiids at 120 kHz. The black irregular line shows the VPR tow-track. The bottom echoes are masked. The color scale on the right indicates the volume back scattering strength, S_v.

sounders and VPR were taken into consideration. For the main towing depth range, where euphausiids were most abundant, this time-lag was estimated to be 180 s for a towing speed of 2 knots and 150 s for 3.5 knots. An acoustic integration layer of 2 m depth range was defined around the VPR-track. The abundance of euphausiids was greatest, within the depth interval of 60–115 m. Data outside this range were therefore excluded from further analysis. To check for any serious effects from patchiness of the euphausiids, time-lags of 80 and 280 s were tested as well as using an integration layer of 5 m. This also served the purpose of investigating whether the use of the wider beam at 38 kHz in 2016 was markedly affecting the results.

Due to the small observation volume of the VPR (407 mL), there was at most a single euphausiid in an image and usually many images without one. To average out this presence/absence effect of the euphausiid detection, 30 s averages of the optic and acoustic values were calculated for the remaining analysis. To minimize further the effect of low values due to possible threshold effects and noise, the data were further reduced by excluding cases where the 30 s acoustic averages of S_{v120} were lower than −80 dB.

As described the VPR was fitted with forward-looking strobe lights, that were either turned on or off and the VPR was towed at different speeds. The data were grouped accordingly into four tow types: type 1: 2 knots/lights off, type 2: 2 knots/lights on, type 3: 3.5 knots/lights off and type 4: 3.5 knots/lights on.

The average back scattering cross section (σ_{bs}), and consequently its logarithmic representation (TS = $10log_{10}(\sigma_{bs})$), at the acoustic frequencies for each year and tow type was estimated as the ratio of the averages of s_v and the number of euphausiids detected by the VPR (ind. m^{-3}). Comparison of σ_{bs} from the different tow types

was used to evaluate the effect of strobe lights and towing speed on the euphausiid density estimated by the VPR.

The above calculation assumes that the isolation of the euphausiid backscatter is functioning effectively. The contribution from copepods to the total backscatter was considered negligible due to their low TS (Stanton and Chu, 2000). The same is assumed for marine snow. The abundance of organisms in the other VPR-derived taxonomic categories was low, and these are hence also assumed to have a negligible contribution to the acoustic backscatter.

Target strength model

For comparison to the target strength estimates derived from VPR and acoustic measurements, euphausiid target strength was also estimated using a Distorted-Wave Born Approximation (DWBA)-based model, representing the shape of the animal as a uniformly bent and slightly tapered cylinder (Stanton *et al.*, 1998; Stanton and Chu, 2000; Lawson *et al.*, 2006). This model involves multiple parameters. The length of the equivalent cylinder was taken as the distance from the anterior tip of the eye to the end of the sixth abdominal segment (Lawson *et al.*, 2006). A correction factor of 0.85 for 2016 and 0.84 for 2018 was used to scale the total lengths (TL) to this acoustic length (AL) based on a subsample of 32 individuals each year. Following the protocols of Lawson *et al.* (Lawson *et al.*, 2006) mean length-to-width ratio (L/w) for the assumed cylindrical shape, measured on the same subsamples, was used, 9.3 for 2016 and 9.4 for 2018. The ratio of the radius of curvature to the length of the cylinder was assumed to be 3 and the taper parameter set to 10 (Lawson *et al.*, 2006), although other than for end-on incidence scattering is mostly insensitive to these parameters when averaging over an assumed ensemble of animals as is done here.

The acoustic material properties of density (g) and sound speed (h) contrasts of *T. raschii* have not been measured for this region and time of year, and so multiple measurements made on *Thysanoessa* species elsewhere were considered, including $g = 1.031$, $h = 1.025$ (Kristensen and Dalen, 1986, measured on *Thysanoessa* species off Norway), $g = 1.04$, $h = 1.026$ (Køgeler *et al.*, 1987, measured on *T. raschii* off Norway), $g = 1.018$, $h = 1.022$ (Lucca *et al.*, 2021, measured on *T. raschii* in the Eastern Bering Sea) and $g = 1.021$, $h = 1.006$ (Smith *et al.*, 2010, measured on *T. raschii* in the Bering Sea).

To account for the fact that the measurements of volume backscattering used to estimate target strength through scaling with VPR measurements of abundance (see above) stem from ensembles of animals, modeled scattering from individual animals was averaged over a distribution of tilt angles. Multiple different possible orientation distributions were considered, including the angles measured directly by the VPR, normal distributions of angles centered close to 0° and with a broad standard deviation of 30°, i.e. N(0°,30°), as measured *in situ* for *T. raschii* and *M. norvegica* by Kristensen and Dalen (Kristensen and Dalen, 1986), and N(5°,39°) measured *in situ* for *T. raschii* in the Eastern Bering Sea by Lucca *et al.* (Lucca *et al.*, 2021), and a narrower distribution centred at a slightly head-up angle (N(9°,4°)), as inferred by McQuinn *et al.* (McQuinn *et al.*, 2013) for *T. raschii*.

Target strengths were estimated using these parametrizations at the survey frequencies of 38, 70, 120 and 200 kHz and are reported as averages (calculated in linear form) over the full net sampled length distributions from Bongo net tows with strobe lights on.

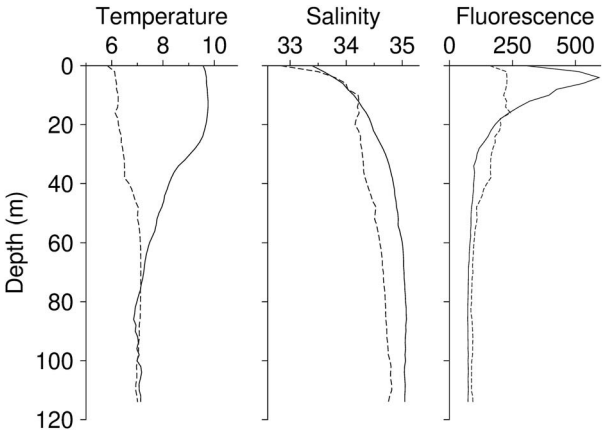

Fig. 3. Vertical distribution of temperature (°C), salinity (PSU) and fluorescence (arbitrary values) in September 2016 (solid lines) and October 2018 (broken lines).

RESULTS

Hydrography

Profiles of temperature, salinity and fluorescence for both years are shown in Fig. 3. In September 2016, temperatures were relatively constant from the surface down to 30 m depth (~9.5°C). Below 30 m depth, temperatures decreased down to ~ 7°C at 80 m. Below 80 m temperatures remained relatively constant (~7°C). In October 2018, temperatures increased more or less steadily from surface (~6°C) to the bottom.

In the depth range of main interest, 60–115 m, the average temperature and salinity was 7.0°C and 35.1 in 2016 and 7.1°C and 34.7 in 2018. The fluorescence integrated over the whole water column was similar for both years (c. 5% difference), but in 2016, the fluorescence in the upper 30 m was higher by a factor of 1.6.

Length distributions of euphausiids from net sampling

Information from the net tows showed that the majority of the euphausiids belonged to *T. raschii* (∼ 96% of all euphausiids in 2016 and 71% in 2018). Two size modes were observed (∼5–10 mm and ∼ 18–27 mm) with the larger mode dominating, especially in tows with the strobe lights activated (Fig. 4). The mean length was 20.7 mm with strobe lights on and 16.7 mm with strobe lights off. In 2018 two modes were observed (∼11–20 and ∼20–27 mm). Mean length was 19.9 mm with strobe lights on and 17.1 mm with lights off. Comparison of the net tows with and without forward-looking lights, resulted in 16- and 13-fold increase in catch in numbers per m^3 using lights in 2016 and 2018, respectively with the increase mainly due to the larger euphausiids.

Abundance and tilt angle distribution of euphausiids from the VPR

Abundance distribution by depth (in 2 m bins) of the euphausiids determined by the VPR-analysis from the two surveys, all tows included, and the volume backscattering coefficient (s_v) at 120 kHz of euphausiids following the VPR tow track are given in Fig. 5. Coefficients of determination (r^2) for the linear regressions between the optic and acoustic data for all frequencies were in all cases 0.9, except for the 120 kHz in 2018 ($r^2 = 0.7$), and with *P*-value less than 0.001. The euphausiids were most abundant in the depth range 60–115 m. Within that depth interval the average density, all tow types included, was estimated to be 130 ind. m^{-3} in 2016 and 176 ind. m^{-3} in 2018. By only including data from tow type 4 (towing speed 3.5 knots and forward-looking strobe lights on), the average density obtained was 297 and 317 ind. m^{-3}. The maximum densities observed within 30 s averages were up to 2 400 ind. m^{-3}. The other most abundant groups within the 60–115 m depth range were copepods (average density of 100 ind. m^{-3} in 2016 and 46 ind. m^{-3} 2018) and marine snow (244 and 194 m^{-3}). Generally, copepods were more numerous where the density of euphausiids was low. All other potential scatterers detected by the VPR were very low in numbers, close to or less than 1 individual m^{-3} (small jellies, Pseudocalanus with egg sacs, Chaetognaths and fish larvae).

For each year, the tilt data from the four VPR tow types were not significantly different at the 95% level ($P > 0.05$), possibly due to not enough observations; hence the tows were combined (Fig. 6). Tilt angles from 893 individual krill images from the 2016 survey were estimated resulting in a mean 0.2° with standard deviation 65°, N(0°,65°). Similarly for 2018, measurements on 394 images gave $\mathcal{N}(-21°,58°)$.

Target strength estimation

The average backscattering cross sections (σ_{bs}) and 95% confidence limits at the different frequencies and years are shown for each tow type in Table II. A highly significant decrease in σ_{bs} from tow type 1 to tow type 4 was found ($P < 0.001$) (Fig. 7). Depending on frequency and year this results in a lowering of the estimated target strength, ranging from 3.8 to 5.1 dB and a mean 4.3 dB. The difference in TS between tow types, using tow type 1 as a reference, is illustrated for 120 and 38 kHz in Fig. 7. The effect of using forward looking lights, irrespective of speed, results in 1.8 dB lower TS. Similarly, increasing tow speed from 2 to 3.5 knots results in 2.3 dB decrease. The decrease with tow type relates to an increase in estimated numerical density, suggestive of avoidance that is mitigated at higher tow speeds and with the use of strobes. The target strength estimates relating to tow type 4 are thus judged to be the most trustworthy due to the apparent reduced avoidance of the krill and are given in the last line for each year in Table III.

Time lags of 80 and 280 s had less than ±0.6 dB effect on the estimated target strength compared to the 150 and 180 s chosen. Using 5 instead of 2 m depth range interval for the acoustic integration had hardly any effect on the volume backscattering strength.

The confidence limits given in Table II only relate to the precision of the acoustic-optic comparison. Uncertainties in the on-axis calibration of the echo sounder and the acoustic and optic volumes are estimated c. 6, 12 and 10%, respectively. Adding those to the confidence limits given in Table II results in uncertainties in the range 18 to 33% with 23% average.

Model calculations of target strength

In Table III, the results from the theoretical computations are given for the different tilt-angle distributions and density and sound speed contrasts. The TS estimates from the VPR-acoustic method are given in the last line for each year. Note that the table presents the target strength averaged over the full length distributions obtained in the Bongo nets (strobe lights on), and thus accounts for both length modes evident in 2018, although the scattering of the smaller mode will be overwhelmed by that of the larger. Modeled target strengths using *g* and *h* by Køgeler *et al.* (Køgeler *et al.*, 1987) and assuming orientation distributions of N(0°,30°) *vs.* N(5°,39°) and N(9°,4°) yield estimates lower by 0.7–1.0 dB and higher by 1.4–3.1 dB, respectively, depending on frequency. Estimates made using the tilt angle distributions observed here with the VPR, N(0°,69°) in September 2016 and N(−21°,58°) in October 2018 are c. 2–3 dB lower.

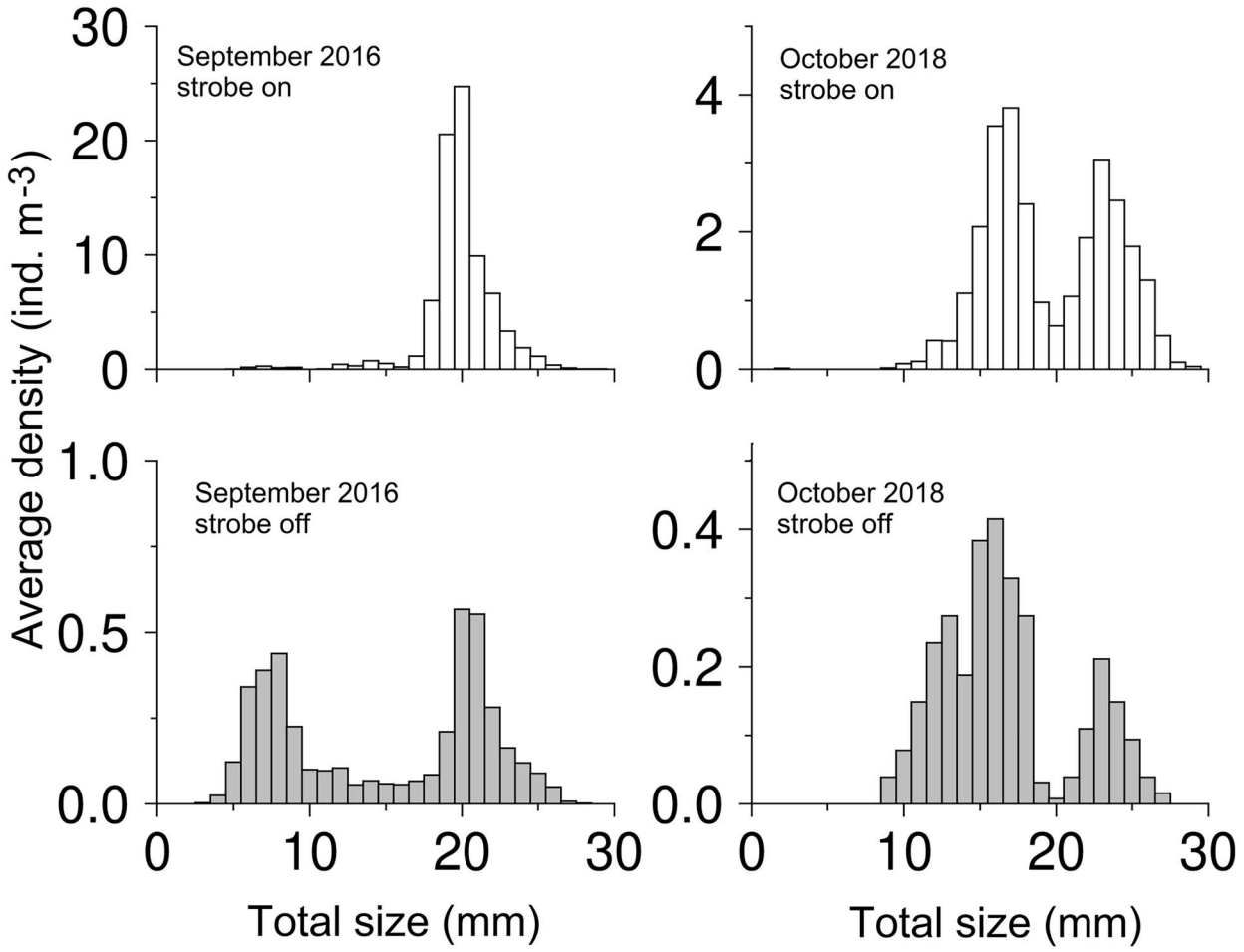

Fig. 4. Length distribution of euphausiids in Bongo-net samples, lower panel obtained with strobe lights off (shaded) and upper panel with strobe lights on. Note the difference in scales on the *Y*-abscissas.

Table II: Backscattering cross sections (σ_{bs}) and the relevant 95% confidence limits for the different frequencies obtained from the VPR-acoustic comparison of the four VPR tow types in 2016 and 2018.

Year/month	Tow speed (knots)	Strobe lights	*N*	$\sigma_{bs} \pm$ 95% confidence limit (10^{-9})			
				38 kHz	70 kHz	120 kHz	200 kHz
2016/September	2.0	off	368	0.46 ± 0.04	1.60 ± 0.14	5.70 ± 0.59	12.63 ± 1.23
	2.0	on	336	0.34 ± 0.03	1.20 ± 0.10	4.49 ± 0.45	9.98 ± 0.92
	3.5	off	229	0.21 ± 0.02	1.04 ± 0.14	3.88 ± 0.65	9.49 ± 1.50
	3.5	on	69	0.14 ± 0.02	0.59 ± 0.11	2.20 ± 0.51	5.28 ± 1.13
2018/October	2.0	off	87	0.42 ± 0.09		3.98 ± 1.14	
	2.0	on	74	0.27 ± 0.06		2.21 ± 0.71	
	3.5	off	235	0.24 ± 0.01		1.94 ± 0.27	
	3.5	on	315	0.16 ± 0.01		1.48 ± 0.14	

The column *N* indicates the number of data, i.e. 30 s averages, for each case.

The lower *g* and *h* measurements made by Kristensen and Dalen (Kristensen and Dalen, 1986); Smith *et al.* (Smith *et al.*, 2010) and Lucca *et al.* (Lucca *et al.*, 2021) give TS values c. 1, 8 and 4 dB lower, respectively. The TS from this work and from some of the above-mentioned model calculations for different density and sound speed contrasts, tilt angle distributions and frequencies are shown in Fig. 8. Generally, the closest match of the

Table III: Results from model-based calculations of euphausiid target strength for different tilt angle distributions and density and sound speed contrasts (g and h).

Year/month	Orientation (Mean, STD)	Density contrast (*g*)	Sound speed contrast (*h*)	TS (dB) 38 kHz	TS (dB) 70 kHz	TS (dB) 120 kHz	TS (dB) 200 kHz
2016/September	N(0°,30°)[a]	1.04[b]	1.026[b]	−100.4	−92.1	−85.4	−80.5
	N(0°,30°)[a]	1.031[a]	1.025[a]	−101.8	−93.4	−86.8	−81.8
	N(0°,30°)[a]	1.021[c]	1.006[c]	−108.0	−99.6	−93.0	−88.2
	N(0°,30°)[a]	1.018[e]	1.022[e]	−104.6	−96.3	−89.1	−84.3
	N(5°,39°)[e]	1.04[b]	1.026[b]	−101.1	−93.0	−86.5	−81.6
	N(9°,4°)[d]	1.04[b]	1.026[b]	−99.1	−89.4	−82.3	−78.2
	N(0°,69°)[f]	1.04[b]	1.026[b]	−102.4	−94.6	−88.3	−83.5
VPR-*acoustic*				*−98.4*	*−92.3*	*−86.6*	*−82.8*
2018/October	N(0°,30°)[a]	1.04[b]	1.026[b]	−100.0		−85.2	
	N(0°,30°)[a]	1.031[a]	1.025[a]	−101.4		−86.6	
	N(0°,30°)[a]	1.021[c]	1.006[c]	−107.6		−92.8	
	N(0°,30°)[a]	1.018[e]	1.022[e]	−104.2		−89.4	
	N(5°,39°)[e]	1.04[b]	1.026[b]	−100.8		−86.3	
	N(9°,4°)[d]	1.04[b]	1.026[b]	−98.4		−82.2	
	N(−21°,58°)[f]	1.04[b]	1.026[b]	−102.0		−88.0	
VPR-acoustic				*−98.2*		*−88.3*	

The last line for each year gives the TS estimates from the VPR-acoustic comparison, representative of tow type 4 (forward looking strobe lights on, towing speed 3.5 knots).
[a]Kristensen and Dalen (Kristensen and Dalen, 1986). [b]Køgeler *et al.* (Køgeler *et al.*, 1987). [c]Smith *et al.* (Smith *et al.*, 2010). [d]McQuinn *et al.* (McQuinn *et al.*, 2013). [e]Lucca *et al.* (Lucca *et al.*, 2021). [f]As estimated from VPR images.

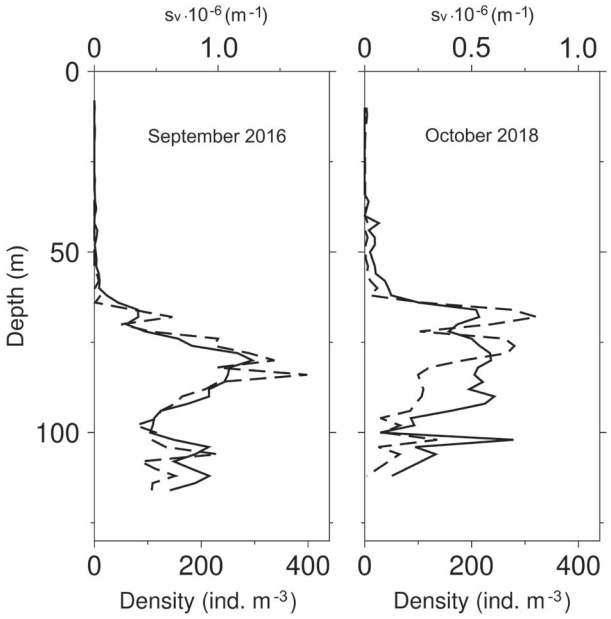

Fig. 5. Vertical profiles of euphausiid density obtained in September 2016 (left panel) and October 2018 (right panel) by the VPR (solid line) and the corresponding euphausiid-classified volume backscattering strength (s_v) at 120 kHz (broken line) in Isafjord-deep. For location see Fig. 1.

modeled and estimated target strength was obtained using tilt angle distribution from either Kristensen and Dalen (Kristensen and Dalen, 1986) or Lucca *et al.* (Lucca *et al.*, 2021) and *g* and *h* reported by Kristensen and Dalen (Kristensen and Dalen, 1986) and Køgeler *et al.* (Køgeler *et al.*, 1987). As expected, using either high *g* and *h* values in combination with narrow tilt angle distributions or low *g* or *h* in combination with wide tilt angle distributions resulted in much higher and lower TS, respectively.

DISCUSSION

The present study shows good agreement between the acoustic and the VPR measurements on relatively homogeneous and mono-specific euphausiid scattering layers and the TS estimates are very similar between surveys at 38 kHz and differ within 2 dB at 120 kHz. At the higher frequencies, 70, 120 and 200 kHz, the TS from this work is in reasonable agreement with the theoretical model, assuming density and sound speed contrasts within the ranges reported by Kristensen and Dalen (Kristensen and Dalen, 1986) and Køgeler *et al.* (Køgeler *et al.*, 1987) and tilt angle distributions within the ranges reported by Kristensen and Dalen (Kristensen and Dalen, 1986) and Lucca *et al.* (Lucca *et al.*, 2021). Similar agreement is obtained when coupling a narrow tilt angle distribution as reported by McQuinn *et al.* (McQuinn *et al.*, 2013) and low *g* and *h* from Lucca *et al.* (Lucca *et al.*, 2021).

Some workers have estimated target strength by scaling acoustic observations to measurements of abundance with nets and compared to theoretical models. In some cases using a narrow tilt angle distribution, the estimated TS has compared favorably with the models, N(0–11°, ≤5°), (McQuinn *et al.*, 2013; Sameoto *et al.*, 1993; Simard and Sourisseau, 2009), while in others using a wider tilt

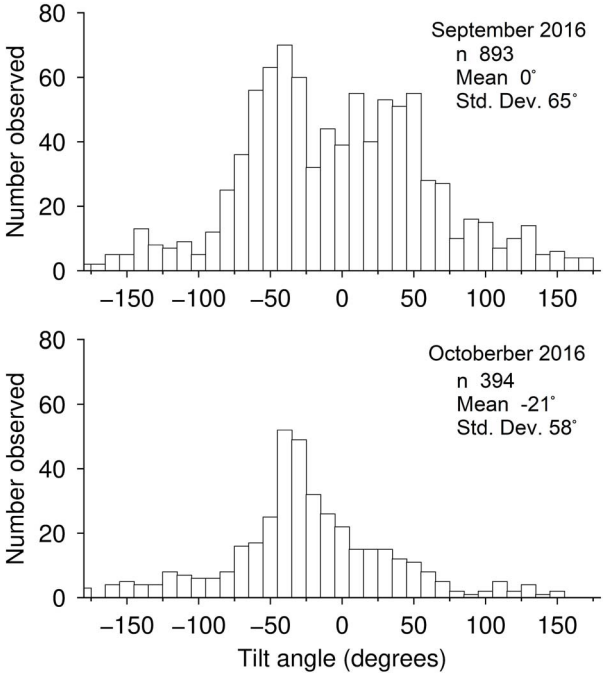

Fig. 6. Tilt-angle distribution of euphausiids from VPR-analysis in September 2016 (upper panel) and October 2018 (lower panel).

angle distribution made a better match, N(0°, 27–30°), (Trevorrow *et al.*, 2005; Wiebe *et al.*, 2013).

Several studies have sought to improve the theoretical physics-based modeling of the target strength of zooplankton (review by Stanton and Chu, 2000; Conti and Demer, 2006 and references therein). The DWBA-based scattering model employed here has compared favorably in previous studies to *in situ* and tank measurements of euphausiids (Stanton *et al.*, 1998; Stanton and Chu, 2000; Lawson *et al.*, 2006). More complicated models of euphausiid scattering are available that account for the stochasticity of sound scattering *via* a random phase element and that implement a more complex two-dimensional shape representation (e.g. Stanton and Chu, 2000; Demer and Conti, 2003a, 2003b; Lucca *et al.*, 2021). When examining ensembles of animals and averaging over a distribution of animal lengths and orientations that include broadside incidence, as is the case here, the effects of such complexities become negligible (Stanton and Chu, 2000) and in the interest of simplicity they were not incorporated here.

The scattering model is sensitive to multiple parameters, notably the length-to-width ratio, contrasts in density and sound speed and tilt angle distributions. Calise and Skaret (Calise and Skaret, 2011) investigated specifically the effect of length-to-width ratio and tilt-angle distribution. Their conclusion, in accordance with several other studies, is that TS-models should be parametrized according to the seasonal variability of krill in the study area. In the present study, length–width measurements were carried out directly on the net samples. Data on density and sound speed contrasts for this study region are lacking. Parametrizing the model using measurements for these parameters made previously on *T. raschii* off Norway (Kristensen and Dalen, 1986; Køgeler *et al.*, 1987), in the Bering Sea (Smith *et al.*, 2010), and Eastern Bering Sea (Lucca *et al.*, 2021) yield differences in TS ranging from 1 to 8 dB, highlighting the substantial variability that surrounds these material property parameters.

The tilt angle distributions as measured by the VPR in this study are quite broad showing a rather strong head-up and head-down tilt of the euphausiids (Fig. 5). Assuming similar towing response of the VPR in the present study as on earlier occasions, the pitch variations (SD = 5.3°) are not expected to have a significant effect on the large standard deviations of tilt angles (SD = 65° and 58°), as measured from the VPR-images. Other studies show close to horizontal *in situ* orientations of *T. raschii* and *M. norvegica* in Norwegian fjords (Kristensen and Dalen, 1986; Kubilius *et al.*, 2015) and of mixed populations of euphausiids in the Eastern Bearing Sea and the Gulf of Alaska (Lucca *et al.*, 2021), although with considerably smaller variance compared to the present study.

Animals with the C-shape, indicative of a tail-flip escape response (Kils, 1981; Hamner and Hamner, 2000; Lawson *et al.*, 2006), were frequently observed in our analysis. It is therefore likely that the euphausiids were to some extent avoiding the VPR in our study. The increased towing speed and forward-looking strobe lights did not significantly alter the observed tilt angle distribution, although this may be due to too few observations. This contrasts with the effect these factors have on the estimated target strength. It is conceivable that although the response of the krill to the VPR may not be effective enough to escape the imaged volume it might well affect its tilt angle, and not only in case of C-shape observations. The observed distributions might relate to animals swimming slightly up or down out of the path of the VPR. It is indeed remarkable, seeing the large effect the forward-looking strobe lights on the net frame have on the catch, increasing it by an order of magnitude (c. 15 fold) that the effect on the numbers of euphausiid imaged by the VPR is less than twofold, considering light effect only. A plausible explanation is that the bright VPR camera flashlight, although side looking, may well screen the oncoming V-fin and camera frame to the euphausiids, and thus reduce the otherwise larger effect of the forward-looking strobe lights.

A source of error is related to the isolation of the euphausiid backscatter from other scatterers. With the

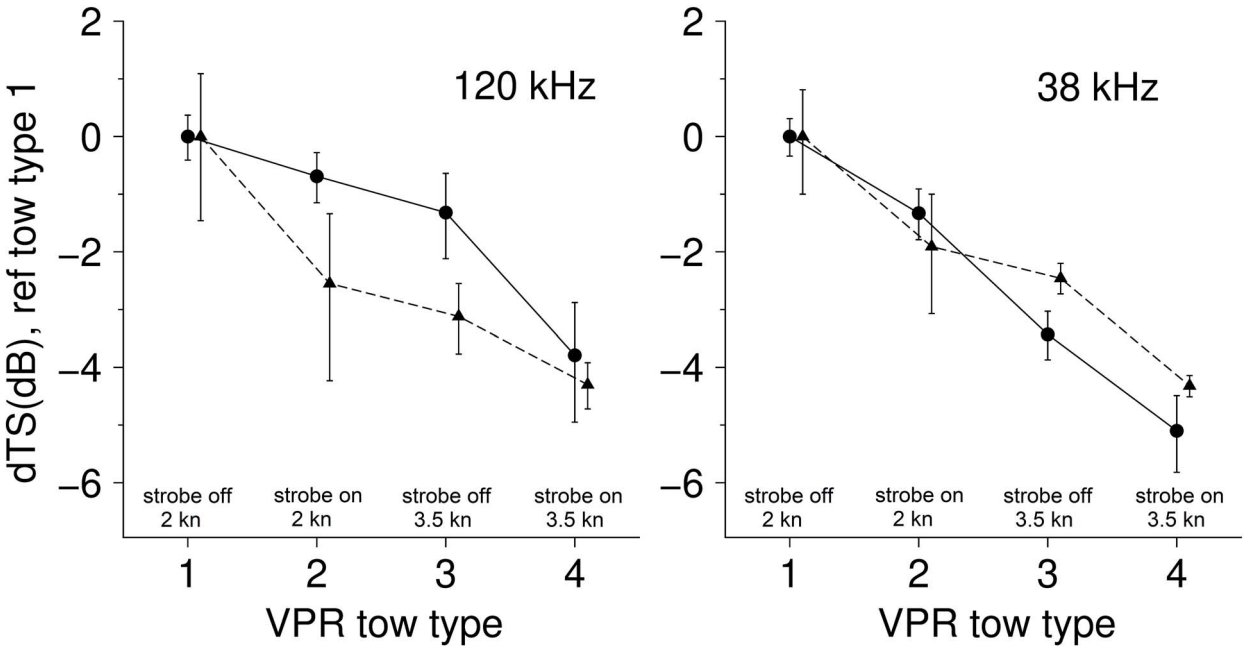

Fig. 7. The difference in TS at 120 and 38 kHz between VPR tow types referred to type 1 tows; (**a**) September 2016 (●, —), and (**b**) October 2018 (▲, —-). The 95% confidence limits shown are valid for the estimated TS according to Table II.

densities of copepods observed by the VPR they would likely affect the estimated TS by less than 0.2 dB. Small scatterers with a frequency response that may increase at the lower frequencies used may be of concern, e.g. small jellies and fish larvae (0-group fish). Although not abundant, if their echoes pass through the classification process, they will affect the lower frequencies considerably. This might to some extent explain the difference observed between the acoustic frequency response of the modeled and measured target strength.

The volume imaged by the VPR directly affects the density of euphausiids as estimated by the VPR. Similarly, the acoustic beam width will affect the backscatter. These two factors will thus have a direct influence on the absolute TS values. Considering that recent transducer models were used, the expected uncertainty is likely less than 0.5 dB, i.e. 12%, (Reynisson, 1998). Calibrations of the optic volume at Seascan and at our laboratory indicate an uncertainty of c. 10%. Oher uncertainties are difficult if not impossible to estimate, relating to the classification process of the echoes, and possible avoidance of the euphausiids to the VPR.

There is a huge difference of the optic and acoustic sampling volumes. The acoustics yields the average of many targets per insonified volume while, even in dense aggregations of euphausiids, the VPR only gives isolated hits. The averaging of the VPR images over 30 s, equivalent to around 350 frames, is an attempt to even this out and the correspondence of the acoustics to the optics is considered credible and the vertical profiles shown in Fig. 5 show a convincing coherence of the data.

Synchronizing the observations of the two instruments in space is critical and depends greatly on the homogeneity of the layers observed. Using different time lags and integration depth intervals did not seriously affect the estimated TS. Accordingly, we believe that the often-observed patchiness of euphausiid distribution detected elsewhere is not seriously affecting the results and that the relatively homogeneous nature of the layers here facilitates the present analysis. This also supports the assumption that using a wider beam transducer at 38 kHz in 2016, having approximately three times the volume of the other transducers, was probably not markedly affecting the results.

CONCLUSION

In summary, we have estimated the average target strength of an ensemble of euphausiids, *T. raschii*, by combining acoustic and VPR measurements and found the target strength at 70, 120 and 200 kHz to agree reasonably well with the theoretical modeling. Such comparison of theoretical modeling of euphausiid acoustic properties to field measurements, whether done by direct acoustic target strength measurements or as done here with other methods, provides enhanced confidence in the estimation of target strength, a crucial quantity for acoustic surveys. The methodological approach of

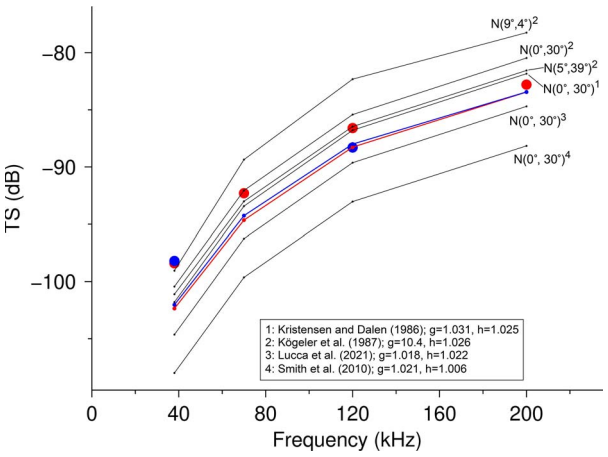

Fig. 8. Target strength estimates from direct estimation based on measured acoustic and VPR data (type 4 tows, strobe on/3.5 kn) and modeling. The 2016 data at 38, 70, 120 and 200 kHz (large red dots) and the 2018 data at 38 and 120 kHz (large blue dots) are shown. The modeled target strength for the VPR-measured orientations, N(0°,65°) in 2016 and N(−21°,56°) in 2018, shown with red and blue lines, using *g* and *h* values according to Køgeler *et al.* (1987). The modeled target strength using various tilt angle distributions: N(0°,30°) (Kristensen and Dalen, 1986), N(9°,4°) (McQuinn *et al.*, 2013) and N(5°,39°) (Lucca *et al.*, 2021) shown with black lines, using *g* and *h* values either according to Kristensen and Dalen (Kristensen and Dalen, 1986); Køgeler *et al.* (Køgeler *et al.*, 1987); Smith *et al.* (Smith *et al.*, 2010); and Lucca *et al.* (Lucca *et al.*, 2021). For the sake of clarity, only the modeled target strength for the 2016 length distribution is shown, except for the measured tilt angle distributions. The modeled TS for the length distributions in 2016 and 2018 are similar, given otherwise identical model parameters, differing only by approximately 0.1–0.6 dB, decreasing with frequency (see Table III).

the present study, relying as it does only on direct acoustic and optic measurements and not requiring the knowledge of orientation distribution, material properties and geometric shape needed by models, provides an attractive alternative to the estimation of euphausiid target strength. Further investigation on how towing speed of a VPR affects the estimated density and tilt angles of euphausiids would be valuable.

DATA AVAILABILITY

The data underlying this article will be shared on request to the corresponding author.

ACKNOWLEDGEMENTS

We would like to thank the crews of the Valur IS-20 and Bjarni Saemundsson RE-30 and Hjalti Karlsson and Einar Hreinsson, MRI, for logistic support and assistance during the cruise. We also would like to thank Solrun Sigurgeirsdottir and Teresa Silva, MRI, for sample analysis. Special thanks go to Mr. Kristjan G. Joakimsson, Hradfrystihusid-Gunnvor Ltd, who supported the project by providing boat with a crew at a very favorable rate. Finally, we thank the anonymous referees for their helpful comments.

FUNDING

This work was partly funded by the AVS Foundation (grant number: R11/12-030-11) and partly by the Marine Research Institute in Iceland. G. Lawson was supported by NOAA Cooperative Agreements NA09OAR4320129 and NA14OAR4320158 through the NOAA Fisheries Quantitative Ecology and Socioeconomics Training (QUEST) program.

REFERENCES

Astthorsson, O. S. (1990) Ecology of the euphausiids *Thysanoessa raschi*, T. *inermis* and *Meganyctiphanes norvegica* in Ísafjord-deep, northwest-Iceland. *Mar. Biol.*, **107**, 147–157. https://doi.org/10.1007/BF01313252.

Astthorsson, O. S. and Gislason, A. (1991) Seasonal abundance and distribution of Caridea larvae in Isafjord-deep, northwest Iceland. *J. Plankton Res.*, **13**, 91–102. https://doi.org/10.1093/plankt/13.1.91.

Astthorsson, O. S. and Gislason, A. (1992) Investigations on the ecology of the zooplankton community in Ísafjord-deep, northwest Iceland. *Sarsia*, **77**, 225–236. https://doi.org/10.1080/00364827.1992.10413508.

Brierley, A. S., Ward, P., Watkins, J. L. and Goss, C. (1998) Acoustic discrimination of Southern Oceanic zooplankton. *Deep Sea Res. Part II: Topical Studies in Oceanography*, **45**, 1155–1173. https://doi.org/10.1016/S0967-0645(98)00025-3.

Calise, L. and Knutsen, T. (2012) Multifrequency target strength of northern krill (*Meganyctiphanes norvegica*) swimming horizontally. *ICES J. Mar. Sci.*, **63**, 1726–1735.

Calise, L. and Skaret, G. (2011) Sensitivity investigation of the SDWBA Antarctic krill target strength model to fatness, material contrast and orientation. *CCAMLR Sci.*, **18**, 97–122.

Chu, D. and Wiebe, P. H. (2005) Measurements of sound-speed and density contrasts of zooplankton in Antarctic waters. *ICES J. Mar. Sci.*, **62**, 818–831. https://doi.org/10.1016/j.icesjms.2004.12.020.

Conti, S. G. and Demer, D. A. (2006) Improved parameterization of the SDWBA for estimating krill target strength. *ICES J. Mar. Sci.*, **63**, 928–935. https://doi.org/10.1016/j.icesjms.2006.02.007.

Coyle, K. O. (2000) Acoustic estimates of zooplankton biomass and distribution: application of canonical correlation to scaling of multifrequency acoustic data. *Can. J. Fish. Aquat. Sci.*, **57**, 2306–2318. https://doi.org/10.1139/f00-155.

Davis, C. S., Hu, Q., Gallager, S. M., Tang, X. and Ashjian, C. J. (2004) Real-time observation of taxa-specific plankton distributions: an optical sampling method. *Mar. Ecol.: Prog. Servir*, **284**, 77–96.

De Robertis, A. (2001) Validation of acoustic echo counting for studies of zooplankton behaviour. *ICES J. Mar. Sci.*, **58**, 543–561.

De Robertis, A., McKelvey, D. R. and Ressler, P. H. (2010) Developement and application of an empirical multifrequency method for backscatter classification in the North Pacific. *Can. J. Fish. Aquat. Sci.*, **69**, 119–130. https:/doi.org/10.1139/F10-075.

Demer, D. A. and Conti, S. G. (2003a) Reconciling theoretical versus empirical target strengths of krill; effects of phase variability on the distorted-wave born-approximation. *ICES J. Mar. Sci.*, **60**, 429–434. https://doi.org/10.1016/S1054-3139(03)00002-X.

Demer, D. A. and Conti, S. G. (2003b) Validation of the stochastic, distorted wave born-approximation model with broadbandwidth, total target-strength measurements of Antarctic krill. *ICES J. Mar. Sci.*, **60**, 625–635. https://doi.org/10.1016/S1054-3139(03)00063-8.

Demer, D. A. and Martin, L. V. (1995) Zooplankton target strength: volumetric or areal dependence? *J. Acoust. Soc. Am.*, **98**, 1111–1118. https://doi.org/10.1121/1.413609.

Einarsson, H. (1945) *Euphausiacea I. Northern Atlantic Species*, Bianco Luno, Copenhagen, p. 191.

Everson, I. (2000) *Krill Biology, Ecology and Fisheries*, Blackwell Science Ltd, Oxford, England.

Everson, I., Tarling, G. A. and Bergström, B. (2006) Improving acoustic estimates of krill: experience from repeat sampling of northern krill (*Meganyctiphanes norvegica*) in Gullmarsfjord, Sweden. *ICES J. Mar. Res.*, **64**, 39–48.

Falk-Petersen, S. and Kristensen, A. (1985) Acoustic assessment of krill stocks in Ullsfjorden, North Norway. *Sarsia*, **70**, 83–90. https://doi.org/10.1080/00364827.1985.10420620.

Foote, K. G., Everson, I., Watkins, J. L. and Bone, D. G. (1990) Target strength of Antarctic krill (*Euphausia superba*) at 38 and 120 kHz. *J. Acoust. Soc. Am.*, **87**, 16–24. https://doi.org/10.1121/1.399282.

Foote, K. G., Knudsen, H. P., Vestnes, G., MacLennan, D. N. and Simmonds, E. J. (1987) Calibration of acoustic instruments for fish density estimates: a practical guide. *ICES Coop. Res. Rep.*, **144**, 1–69.

Foote, K. G. and MacLennan, D. N. (1984) Comparison of copper and tungsten carbide calibration spheres. *J. Acoust. Soc. Am.*, **75**, 612–616. https://doi.org/10.1121/1.390489.

Gislason, A., Petursdottir, H. and Reynisson, P. (2022) Effect of strobe lights on catches and length distributions of euphausiids collected by Bongo nets. *J. Plankton Res.* 1–11. https://doi.org/10.1093/plankt/fbac063.

Greene, C. H., Stanton, T. K., Wiebe, P. H. and McClatchie, S. (1991) Acoustic estimates of Antarctic krill. *Nature*, **349**, 110. https://doi.org/10.1038/349110a0.

Hamner, W. M. and Hamner, P. P. (2000) Behavior of Antarctic krill (*Euphausia superba*): schooling, foraging, and antipredatory behavior. *Can. J. Fish. Aquat. Sci.*, **57**, 192–202. https://doi.org/10.1139/f00-195.

Hemple, G. (1983) FIBEX—an international survey in the Southern Ocean: review and outlook. *Mem. Natl. Inst. Polar Res. Special Issue*, **27**, 1–15.

Hewitt, R. P. and Demer, D. A. (1993) Dispersion and abundance of Antarctic krill in the vicinity of Elephant Island in the 1992 austral summer. *Mar. Ecol. Prog. Ser.*, **99**, 29–39. https://doi.org/10.3354/meps099029.

Hewitt, R. P. and Demer, D. A. (1996) Lateral target strength of Antarctic krill. *ICES J. Mar. Sci.*, **53**, 297–302. https://doi.org/10.1006/jmsc.1996.0038.

Hewitt, R. P. and Demer, D. A. (2000) The use of acoustic sampling to estimate the dispersion and abundance of euphausiids, with an emphasis on Antarctic krill, *Euphausia suberba*. *Fish. Res.*, **47**, 215–229. https://doi.org/10.1016/S0165-7836(00)00171-5.

Hu, Q. and Davis, C. S. (2006) Accurate automatic quantification of taxa-specific plankton abundance using dual classification with correction. *Mar. Ecol. Prog. Ser.*, **306**, 51–61. https://doi.org/10.3354/meps306051.

Kils, U. (1981) The swimming behavior, swimming performance and energy balance of Antarctic krill, *Euphauisa superba*. *BIOMASS Scientific Series*, **3**, 1–121.

Klevjer, T. H. and Kaartvedt, S. (2006) In situ target strength and behaviour of northern krill (*Meganyctiphanes norvegica*). *ICES J. Mar. Sci.*, **63**, 1726–1735. https://doi.org/10.1016/j.icesjms.2006.06.013.

Køgeler, J. W., Falk-Petersen, S., Kristensen, Å., Pettersen, F. and Dalen, J. (1987) Density and sound speed contrasts in sub-Arctic Zooplankton. *Polar Biol.*, **7**, 231–235. https://doi.org/10.1007/BF00287419.

Korneliussen, R. J. (2000) Measurements and removal of echo integration noise. *ICES J. Mar. Sci.*, **57**, 1204–1217. https://doi.org/10.1006/jmsc.2000.0806.

Korneliussen, R. J., Diner, N., Ona, E., Berger, L. and Fernandes, P. G. (2008) Proposals for the collection of multifrequency acoustic data. *ICES J. Mar. Sci.*, **65**, 982–994. https://doi.org/10.1093/icesjms/fsn052.

Korneliussen, R. J. and Ona, E. (2002) An operational system for processing and visualizing multi-frequency acoustic data. *ICES J. Mar. Sci.*, **59**, 293–313. https://doi.org/10.1006/jmsc.2001.1168.

Korneliussen, R.J., Ona, E., Eliassen, I., Heggelund, Y., Patel, P., Godø, O.R., Giertesen, C. and Patel *et al.* (2006) The large scale survey system-LSSS. *Proceedings of the 29th Scandinavian Symposium on Physical Acoustics*, Ustaoset 29 January–1 February. https://marec.no/references/proceedingsUstaoset2006_Korneliussen_etal_LSSS.pdf.

Kristensen, Å. and Dalen, J. (1986) Acoustic estimation of size distribution and abundance of zooplankton. *J. Acoust. Soc. Am.*, **80**, 601–611. https://doi.org/10.1121/1.394055.

Kubilius, R., Ona, E. and Calise, L. (2015) Measuring in situ krill tilt orientation by stereo photogrammetry: examples for *Euphausia suberba* and *Meganyctiphanes norvegica*. *ICES J. Mar. Sci.*, **72**, 2494–2505. https://doi.org/10.1093/icesjms/fsv077.

Lawson, G. L., Wiebe, P. H., Ashjian, C. J., Chu, D. and Stanton, T. K. (2006) Improved parameterization of Antarctic krill target strength models. *J. Acoust. Soc. Am.*, **119**, 232–242. https://doi.org/10.1121/1.2141229.

Logerwell, E. A. and Wilson, C. D. (2004) Species discrimination of fish using frequency-dependent acoustic backscatter. *ICES J. Mar. Sci.*, **61**, 1004–1013. https://doi.org/10.1016/j.icesjms.2004.04.004.

Lucca, B. M., Ressler, P. H., Harvey, H. R. and Warren, J. D. (2021) Individual variability in sub-Arctic krill material properties, lipid composition, and other scattering model inputs affect acoustic estimates of their population. *ICES J. Mar. Sci.*, **78**, 1470–1484. https://doi.org/10.1093/icesjms/fsab045.

MacLennan, D. N., Fernandes, P. G. and Dalen, J. (2002) A consistent approach to definitions and symbols in fisheries acoustics. *ICES J. Mar. Sci.*, **59**, 365–369. https://doi.org/10.1006/jmsc.2001.1158.

Martin Traykovski, L. V., O'Driscoll, R. L. and McGehee, D. E. (1998) Effect of orientation on broadband acoustic scattering of Antarctic krill *Euphausia superba*: Implications for inverting zooplankton spectral acoustic signatures for angle of orientation. *J. Acoust. Soc. Am.*, **104**, 2121–2135. https://doi.org/10.1121/1.423726.

Mauchline, J. and Fisher, L. R. (1969) In Russell, S. F. S. and Yonge, S. M. (eds.), *The Biology of Euphausiids*, Academic Press, London and New York.

McGehee, D. E., O'Driscoll, R. L. and Martin Traykovski, L. V. (1998) Effects of orientation on acoustic scattering from Antarctic krill at 120 kHz. *Deep-Sea Res. II Top. Stud. Oceanogr.*, **45**, 1273–1294. https://doi.org/10.1016/S0967-0645(98)00036-8.

McQuinn, I. H., Dion, M. and St. Pierre, J.-F. (2013) The acoustic multifrequency classification of two sypatric euphausiid species (*Meganyctiphanes norvegica* and *Thysanoessa raschii*), with empirical SDWBA model validation. *ICES J. Mar. Sci.*, **70**, 636–649. https://doi.org/10.1093/icesjms/fst004.

Miyashita, K., Aoki, I. and Inagaki, T. (1996) Swimming behaviour and target strength of Isada krill (*Euphausia pacifica*). *ICES J. Mar. Sci.*, **53**, 303–308. https://doi.org/10.1006/jmsc.1996.0039.

Motoda, S. (1959) Devices of simple plankton apparatus. *Mem Fac Fish Hokkaido Univ*, **7**, 73–94.

Pauly, T. and Penrose, J. D. (1998) Laboratory target-strength measurements of free-swimming Antarctic krill (*Euphausia superba*). *J. Acoust. Soc. Am.*, **103**, 3268–3280. https://doi.org/10.1121/1.423077.

Reiss, C. S., Cossio, A. M., Loeb, V. and Demer, D. A. (2008) Variations in the biomass of Antarctic krill (*Euphausia superba*) around the South Shetland Islands, 1996–2006. *ICES J. Mar. Sci.*, **65**, 497–508. https://doi.org/10.1093/icesjms/fsn033.

Ressler, P. H., Brodeur, R. D., Peterson, W. T., Pierce, S. D., Vance, P. M., Røstad, A. and Barth, J. A. (2005) The spatial distribution of euphausiid aggregations in the Northern California Current during August 2000. *Deep-Sea Res. II Top. Stud. Oceanogr.*, **52**, 89–108. https://doi.org/10.1016/j.dsr2.2004.09.032.

Reynisson, P. (1998) Monitoring of equivalent beam angles of hull-mounted acoustic survey transducers in the period 1983–1995. *ICES J. Mar. Sci.*, **55**, 1125–1132. https://doi.org/10.1006/jmsc.1998.0369.

Reynisson, P. and Gislason, A. (2015) Bergmálsmælingar á ljósátu við Ísland árin 2011–2014 (Acoustic measurements of euphausiids around Iceland 2011–2014). *Hafrannsóknir*, **181**, 26–35.

Sakinan, S., Lawson, G. L., Wiebe, P. H., Chu, D. and Copley, N. J. (2019) Accounting for seasonal and composition-related variability in acoustic material properties in estimating copepod and krill target strengt. *Limnol. Oceanogr. Methods*, **17**, 607–625. https://doi.org/10.1002/lom3.10336.

Sameoto, D. (1980) Quantitative measurements of euphausiids using a 120-kHz sounder and their in situ orientatin. *Can. J. Fish. Aquat. Sci.*, **37**, 693–702. https://doi.org/10.1139/f80-087.

Sameoto, D., Cochrane, N. and Herman, A. (1993) Convergence of acoustical, optical and net-catch-estimates of eupausiids abundance: use of artificial light to reduce net avoidance. *Can. J. Fish. Aquat. Sci.*, **50**, 334–346. https://doi.org/10.1139/f93-039.

Silva, T., Gislason, A., Astthorsson, O. S. and Marteinsdottir, G. (2016) Abundance and distribution of early life stages of krill around Iceland during spring. *Mar. Biol. Res.*, **12**, 864–873. https://doi.org/10.1080/17451000.2016.1210808.

Simard, Y. and Lavoie, D. (1999) The rich krill aggregation of the Saguenay—St. Lawrence Marine Park: hydroacoustic and geostatistical biomass estimates, structure, variability, and significance for whales. *Can. J. Fish. Aquat. Sci.*, **56**, 1182–1197. https://doi.org/10.1139/f99-063.

Simard, Y. and Sourisseau, M. (2009) Diel changes in acoustic and catch estimates of krill biomass. *Can. J. Fish. Aquat. Sci.*, **66**, 1318–1325.

Smith, J. N., Ressler, P. H. and Warren, J. D. (2010) Material properties of euphausiids and other zooplankton from the Bering Sea. *J. Acoust. Soc. Am.*, **128**, 2664–2680. https://doi.org/10.1121/1.3488673.

Stanton, T. K. and Chu, D. (2000) Review and recommendations for the modelling of acoustic scattering by fluid-like elongated zooplankton: euphausiids and copepods. *ICES J. Mar. Sci.*, **57**, 793–807. https://doi.org/10.1006/jmsc.1999.0517.

Stanton, T. K., Chu, D. and Wiebe, P. H. (1998) Sound scattering by several zooplankton groups. II. Scattering models. *J. Acoust. Soc. Am.*, **103**, 236–253. https://doi.org/10.1121/1.421110.

Trevorrow, M. V., Mackas, D. L. and Benfield, M. C. (2005) Comparison of multifrequency acoustic and in situ measurements of zooplankton abundances in Knight Inlet, British Columbia. *J. Acoust. Soc. Am.*, **117**, 3574–3588. https://doi.org/10.1121/1.1920087.

Wiebe, P. H., Allison, D., Kennedy, M. and Moncoiffé, G. (2015) A vocabulary for the configuration of net tows for collecting plankton and micronekton. *J. Plankton Res.*, **37**, 21–27. https://doi.org/10.1093/plankt/fbu101.

Wiebe, P. H., Ashjian, C., Gallager, S., Davis, C., Lawson, G. and Copley, N. (2004) Using a high-powered strobe ligth to increase the catch of Antarctic krill. *Mar. Biol.*, **144**, 493–502. https://doi.org/10.1007/s00227-003-1228-z.

Wiebe, P. H., Greene, C. H., Stanton, T. K. and Burczynski, J. (1990) Sound scattering by live zooplankton and micronekton: empirical studies with a dual-beam acoustical system. *J. Acoust. Soc. Am.*, **88**, 2346–2360. https://doi.org/10.1121/1.400077.

Wiebe, P. H., Lawson, G. L., Lavery, A. C., Copley, N. J., Horgan, E. and Bradley, A. (2013) Improved agreement of net and acoustical methods for surveying euphausiids by mitigating avoidance using a net-based LED strobe light system. *ICES J. Mar. Sci.*, **70**, 650–664. https://doi.org/10.1093/icesjms/fst005.